

tra to a common intensity scale (no scaling in intensity was made here), and that there is no significant detector non-linearity present (which would be manifest as residual differences at the positions of strong lines). Furthermore, the difference of the spectra has an rms noise very near to the calculated photon shot noise limit, given the quoted 6.8 electron/ADU calibration.

From these and other results from the run it is clear that apparent S/N ratios of 300 : 1 are achievable with this detector. Higher ratios may be possible with multiple integrations.

The only serious problem found in our data is shown in Figure 2b. The two columns marked there consistently show residuals (data-minus-fit) dependent on signal level. We understand (Sandro D'Odorico, private comm.) that these RCA chips are known to exhibit such behaviour – that is, to have occasional column pairs in which part of the signal in one column seems to end up in the adjacent column, when the signal is above some threshold level. We have experimented with trying to fix this problem by applying an interpolated re-transfer of signal after the fact, but could not convince ourselves that the results were always reliable.

Our solution to the problem is to mask the offending columns of data away, and exclude them from the template fitting process. We thereby lose some 15% of our signal, which we deem an

acceptable loss to guarantee the quality of the photometry. The data in Figure 3 were processed with these columns masked away.

One negative side effect results, however. With two fewer signal columns, the fitting algorithm now no longer effectively ignores the single pixel outliers due to particle detections. We have had to include a routine, therefore, to test for pixels more than 5 times the (*a priori* known) noise sigma from the fit, and throw the worst single one out. Although not particularly elegant, this strategy has proven very effective in removing particle detections.

Focus Effects

Our data-minus-fit residual frames are exquisitely sensitive to focus variations along the spectra (although the final integrated intensities at each point should not be). We find that the width of the spectra does vary, being broadest at the two ends, but that the effect is so small that we cannot measure it in the widths of individual emission lines in the calibration spectra. We suppose that a small tilt of the CCD with respect to the focal plane of a half degree is sufficient to give the magnitude of what we see. From the residual frames we infer that over about a quarter of the total length of the recorded data, the instrumental profile is clearly constant enough for use

in spectral modelling analysis with a single model profile. But of course, the derivation of the appropriate profile remains problematical.

Conclusions

Based on our, admittedly incomplete, analysis, we feel we can make the following conclusions.

(i) The double density RCA CCD on the CES long camera works very well, even at 4000 Å.

(ii) Its lower noise per pixel compared to the Reticon, and its registry of each spectral channel with multiple pixels, allows particle detections to be discovered and easily removed.

(iii) The expected quantum noise limit is achieved on single integrations, allowing S/N ratios of several hundred to be obtained. We have not done tests to determine whether S/N ratios of 1,000 and greater are possible, by summing multiple integrations.

(iv) Photometrically unacceptable columns on the detector have been discovered, which should be masked out during analysis if results of the highest quality are to be attained.

(v) Least squares fitting of templates for data extraction, and probably also for wavelength calibrations, seems a good way to determine the length of spectrum over which the instrumental profile is sensibly constant in shape.

What is the Mass-to-Light Ratio of the Old Magellanic Globular Cluster NGC 1835?

G. MEYLAN, ESO

P. DUBATH, M. MAYOR, Observatoire de Genève, Switzerland, and

P. MAGAIN, Institut d'Astrophysique de Liège, Belgium

1. Richness of the Southern Sky

We astronomers are lucky: our Galaxy has two companion galaxies, the Large and Small Magellanic Clouds, situated well above the galactic plane, which contain a huge potential of astrophysical information. For example, concerning star clusters, the realm of the globular clusters is much richer and more varied in the Magellanic Clouds than in the Galaxy: rich clusters of all ages are observed, from the youngest, having ages of a few tens 10^6 yr, to the oldest, having ages of the order or larger than 10^{10} yr. In this paper, only old Magellanic and galactic globular clusters are considered.

From the determinations found in the literature of the individual masses of the richest old clusters, a systematic difference seems to exist between the globulars in our Galaxy and in the Magellanic Clouds, Magellanic clusters appearing lighter than galactic clusters. This difference in mass between old rich Magellanic and galactic clusters obviously has direct consequences on the mass-to-light ratio determination of the considered clusters, reflecting perhaps systematic differences in mass function. This was challenged and discussed recently (Meylan 1988b). A way to resolve this controversy consists in obtaining good observational values of the central

velocity dispersion, by detecting the very small line broadening present in the integrated light spectra.

2. Magellanic and Galactic M/L_v Ratio

2.1 Magellanic globular clusters

The method most often used for obtaining the total mass of Magellanic clusters is related to the systemic rotation of the Magellanic Clouds. The observed value of the tidal radius r_t of the cluster is transformed into mass, in a way similar to the case of galactic open clusters. It is assumed that the clusters

are in rotation along circular orbits around the centre of mass of the Clouds, the old clusters seeming to form a disk-like system in the LMC. Tidal masses, particularly for the outer clusters, may be underestimated, if these clusters are in radial rather than circular orbits.

Observational determinations of the tidal radii by star counts in the outer parts of Magellanic clusters is pioneer work of a difficult nature, since the pollution by Magellanic field stars still induces uncertainties. Determination of tidal radius is a difficult task even for the galactic globular clusters, and the “observed limiting radius” determinations are rather weak for nearly all of them.

Using the above method, Elson and Freeman (1985) found for the following three old LMC clusters, NGC 1835, NGC 2210, and NGC 2257, total masses equal to, respectively, $M_{\text{tot}} = 7.3, 1.9,$ and $3.7 \cdot 10^4 M_{\odot}$, with corresponding mean M/L_v ratios equal to 0.18, 0.11 and 0.56 (Table 1).

Reasonably good dynamical constraints – surface brightness profile and central value of the velocity dispersion – have been published so far only for one Magellanic cluster: NGC 1835. It is only in the case of this cluster that the determination of the velocity dispersion ($\sigma(V_r) = 5 \text{ km s}^{-1}$, obtained by Elson and Freeman (1985) from a Fourier method applied to integrated light spectra) can be converted into mass, by using the core radius and the dimensionless mass derived from the fit of the observed surface brightness profile to single-mass isotropic King models. Elson and Freeman (1985) find for NGC 1835, $M_{\text{tot}} = 1.6 \cdot 10^5 M_{\odot}$, with $M/L_v = 0.42$ (Table 1).

All the former mass and mass-to-light ratio determinations concerning NGC 1835 (Freeman 1974, Chun 1978, Elson and Freeman 1985, and Meylan 1988b) are displayed in Table 1 and will be discussed in Section 4 with the results of the present study.

2.2 Galactic globular clusters

In our Galaxy, only six globular clusters have been studied so far with King-Michie multi-mass anisotropic dynamical models, consisting of about ten different subpopulations. The observational constraints for such models are the surface brightness in the central parts and star counts in the outer regions, with in addition the high quality radial velocities for numerous individual member stars. These six best studied galactic globular clusters are M3 (Gunn and Griffin 1979), M92 (Lupton et al. 1985), M2 (Pryor et al. 1986), M13 (Lupton et al. 1987), ω Cen (Meylan 1987), and 47 Tuc (Meylan 1988a, 1989). Apart

TABLE 1: The different values of the total mass of NGC 1835 published during these last 15 years.

Year	x	M_{tot} [$10^6 M_{\odot}$]	M/L_v [\odot units]	r_a [r_c]	Authors
1974	...	0.045	0.2	...	Freeman 1974
1978	...	0.044	0.12	...	Chun 1978
1978	...	0.062	0.17	...	Chun 1978
1985	...	0.073	0.18	...	Elson & Freeman 1985
1985	...	0.16	0.42	iso	Elson & Freeman 1985
1988	1.75	0.39	1.30	iso	Meylan 1988b
1988	1.50	0.28	0.94	30	Meylan 1988b
1989	1.25	1.03	3.58	iso	present study
1989	1.00	0.81	2.83	30	present study

from ω Cen, the (unique) giant cluster of the Galaxy ($M_{\text{tot}} = 3.9 \cdot 10^6 M_{\odot}$), the total masses range from 0.4 to $1.1 \cdot 10^6 M_{\odot}$, whereas all the mass-to-light ratios are located between about 2 and 3. The above values can be considered as typical of the masses and mass-to-light ratios of the rich globulars of our Galaxy.

2.3 A difference in M/L_v by a factor of 10?

The typical mass of the globular clusters in the Clouds (less than $10^5 M_{\odot}$) is smaller than the typical mass of the globular clusters in the Galaxy (greater than $10^5 M_{\odot}$). This difference in mass between rich galactic and Magellanic clusters obviously has direct consequences on the mass-to-light ratio: $M/L_v = 0.1-0.5$ for those in the Magellanic Clouds and $M/L_v = 2.0-3.0$ for those in the Galaxy. Is there a genuine systemic difference in M/L_v , by nearly a factor of 10?

It is worth emphasizing that the above question does not only concern globular clusters. For example, despite the range of a factor of 1,000 in galaxy luminosities in the Local Group galaxies, the globular cluster luminosity distributions of these galaxies are consistent with being of the same form in all of them. It is generally accepted that the globular cluster population in galaxies was formed with the same distribution of globular cluster masses and luminosities in all galaxies. A clear systematic difference in M/L_v between Magellanic and galactic globular cluster populations would cast doubt as to their use as secondary distance indicators in the cosmological distance ladder.

At the present time, there is no definitive answer. We emphasize that only the rich old globular clusters in the Magellanic Clouds and in the Galaxy are considered here. It is essential to realize that any comparison between the M/L_v values of these two populations is so far strongly hampered by the fact that these values proceed from different determi-

nation processes. Comparison between galactic and Magellanic M/L_v values should be done only between results coming from the same kind of models constrained by the same kind of observational data. The more elaborated King-Michie dynamical models have been applied so far only to galactic globular clusters (with the exception of NGC 1835), due to the lack of observational data concerning the Magellanic clusters.

This situation is on the verge of change: if it is still difficult to obtain velocity dispersion profiles of Magellanic clusters, it appears now feasible to obtain at least the central value of the velocity dispersion, from integrated light spectra. The obtaining of such an essential observational constraint, in the case of the old Magellanic globular NGC 1835 is presented below, with a discussion of the application of this new result to a King-Michie model and the consequences on the M/L_v ratio concerning this cluster.

3. Core Velocity Dispersion from Cross-Correlation Technique

3.1 Optical and numerical cross-correlations

For more than twenty years, the cross-correlation spectroscopy has proven its exceptional efficiency in radial velocity determination (Griffin 1967, Baranne, Mayor, and Poncet 1979). The cross-correlation between a stellar spectrum and a template allows to condense the radial velocity information, contained in the stellar spectrum, into the equivalent of a single spectral “line”: the cross-correlation function. For example, with the two CORAVEL spectrometers, using simultaneously about 1,500 spectral lines, a few minutes of integration provide a determination of the radial velocity of a 14th V-magnitude star with a precision of about 1 km s^{-1} .

In such spectrometers, the cross-correlation is done optically, but it is easy to

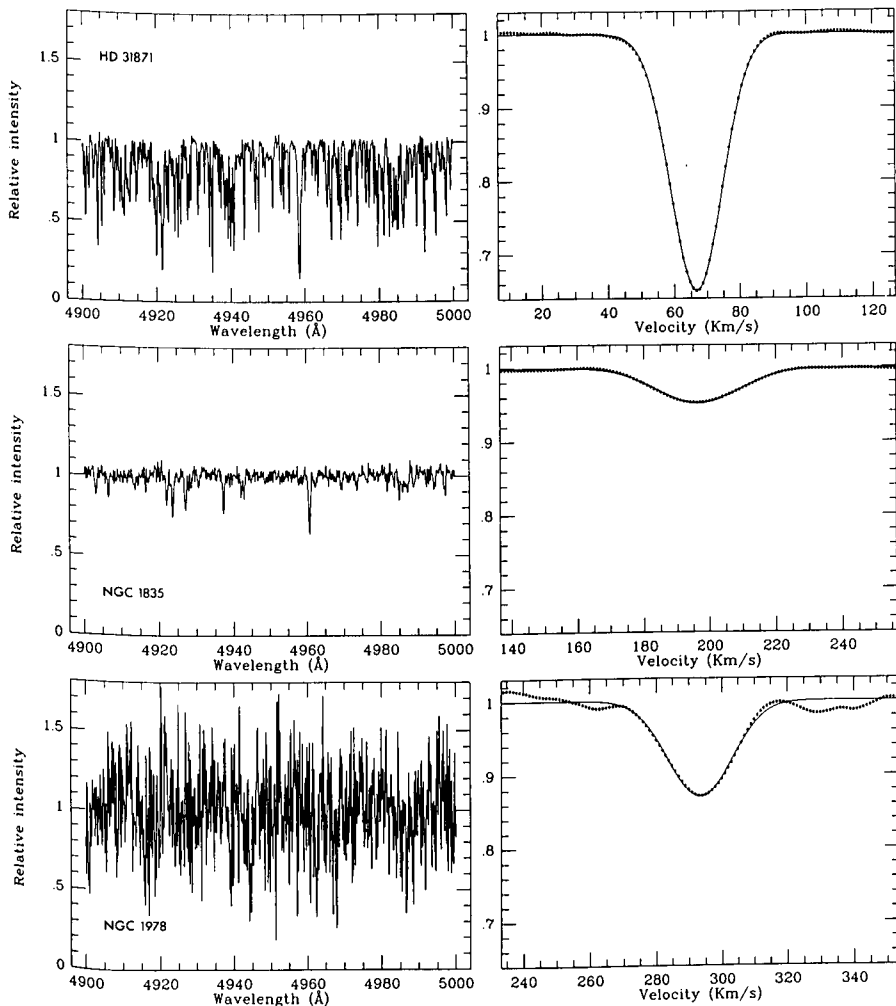


Figure 1: Left: for the comparison star HD 31871 (K5 III, $m_v = 9$), and for the two old LMC globular clusters NGC 1835 and NGC 1978, 100 Å ranges from the spectra obtained with CASPEC (Cassegrain ESO Echelle Spectrograph mounted on the ESO 3.6-m telescope at La Silla) are displayed. Right: numerical cross-correlation functions for the same three objects; due to their low metallicities, the cross-correlation functions of the two clusters are much less contrasted than the cross-correlation function of the comparison star.

visualize obtaining the same result from a numerical correlation between registered spectra. Such radial velocity measurements are obtained by D. Latham (CfA) and his collaborators, from numerical cross-correlation of registered spectra having a wavelength range of 50 Å. A numerical cross-correlation, using CASPEC spectra, would take advantage of a much larger spectral range (larger than 1000 Å). The numerical cross-correlation gives *a priori* a noticeable gain: the scanning required to build optically the cross-correlation function on the telescope is no longer necessary, providing an immediate gain of about 2.5 magnitudes. In addition, we can expect some further gain due to the high quantum efficiency of CCDs as compared to photomultipliers. Unfortunately the readout noise of the CCD is still the limiting factor.

If the cross-correlation spectroscopy is well adapted to radial velocity determinations, it shows the same efficiency

concerning line broadening measurements, giving access to rotation through precise $V \sin i$. Even more, the cross-correlation function of the integrated light spectra of globular cluster cores should allow a determination of the velocity dispersion of the stars in these cores. A resolution of about 20,000 is needed to have access through cross-correlation spectroscopy to Doppler broadenings of a few km s^{-1} , but a low signal-to-noise ratio (as low as 2-3) will be admissible. A similar approach was already used by G. Illingworth in 1976, to determine the velocity dispersion in the nucleus of a few galactic globular clusters, using Fourier transforms of integrated light spectra (on photographic plates).

3.2 Results from observations during a test night

In order to investigate the possibilities of CASPEC spectra applied to this tech-

nique, we obtained two hours of a test night at the ESO 3.6-m telescope. Spectra were obtained for two old globular cluster nuclei of the Large Magellanic Cloud as for two K5 III comparison stars. The integration times were two 20-minute exposures for NGC 1978 and two 30-minute exposures for NGC 1835. Due to the large difference in central surface brightness between the two clusters, the signal-to-noise ratio of the two cluster spectra are quite different (Fig. 1). The case of NGC 1978 is especially interesting for illustrating the potentialities of the method: the spectrum of this cluster has only a signal-to-noise ratio of about 2.

To increase the sensitivity to line broadening, we prefer to exclude strong saturated lines in the correlation process and use only small unsaturated lines selected from the CORAVEL template (here using its numerical version). Only the spectral domain of the CORAVEL mask between 4400 and 5200 Å has been used when cross-correlating CASPEC spectra with the numerical mask. In the left half of Figure 1, 100 Å ranges from the spectra of one comparison star (HD 31871, K5 III, $m_v = 9$) and from the two clusters NGC 1835 and NGC 1978 are displayed. In the right half of the same figure the cross-correlation functions obtained for these objects are plotted. Due to their low metallicities, the cross-correlation functions of the two clusters are much less contrasted than the cross-correlation functions of the two comparison stars (the width of the cross-correlation function does not depend on the metallicity!). After normalization of the cross-correlation function of the cluster NGC 1835 in order to have the same depth as the cross-correlation function of the comparison star (Fig. 2), we immediately notice the important broadening of the cluster cross-correlation function. Both comparison stars have been checked by direct CORAVEL measurements to have an almost zero rotation. Consequently, the velocity dispersion in the core of NGC 1835 is immediately derived:

$$\sigma_v(\text{NGC 1835}) = 10.1 \text{ km s}^{-1}$$

During the integration, a scanning of the nucleus was done with the entry slit, in order to cover a zone of 6×6 arcsec, so that the velocity dispersion is based on the light coming from more than 100 giant stars. Data reduction of the spectra was done with MIDAS. It is worth mentioning that the cross-correlation technique allows us to determine accurately a broadening of only a few per cent of the FWHM of the cross-correlation function (at zero broadening factor,

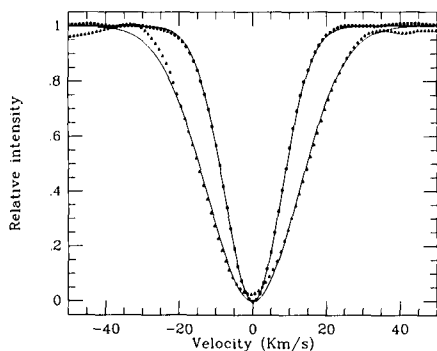


Figure 2: Normalized cross-correlation functions of the cluster NGC 1835 (triangles) and of the comparison star HD 31871 (dots); the continuous lines are the corresponding fitted gaussians; the important broadening of the cluster cross-correlation function is conspicuous and allows an immediate determination of the velocity dispersion in the core of NGC 1835: $\sigma(V_r) = 10.1 \text{ km s}^{-1}$.

the FWHM of the CASPEC cross-correlation function is equivalent to about 18 km s^{-1} , the pixel size being 9 km s^{-1}).

4. NGC 1835 M/L_V from King-Michie Model

4.1 Observational constraints

With this new determination for the velocity dispersion in the core of the old LMC globular cluster, $\sigma(V_r) = 10.1 \text{ km s}^{-1}$, it is possible to constrain King-Michie dynamical models. The other observational constraint, viz. the surface brightness profile, is a composite profile – namely CCD surface brightness photometry in the very central parts, centred aperture photometry and drift scan measures in the central and intermediate parts, and star counts in the outer parts – obtained by mixing Elson and Freeman (1985) and Mateo (1987) data (already used in Meylan 1988b).

Figure 3 displays the surface brightness profiles, as a function of the radius, of the observations and of one of the 8 best models (lowest reduced χ^2_ν) obtained from a grid of about 400 models. The model profile, integrated along the line-of-sight, concerns only the sub-population containing giants, subgiants, and stars at the top of the main sequence, i.e. all the stars emitting most of the light of the cluster. The residuals between observations (dots) and model (continuous line) are also displayed in the lower part of the same figure.

4.2 Mass function exponent, total mass, and mass-to-light ratio

The models are calculated by using the same mass function exponent x ($dN \propto m^{-x} d\log(m)$) for the entire range in stellar mass, i.e. from 0.1 to $100 M_\odot$.

Within the large range of values of x investigated (from 0.0 to 3.5 by steps of 0.25), only the values between 1.00 and 1.75 provide models able to fit the observations. Only models with small fractions of stellar remnants (neutron stars and white dwarfs) fit the observations: the fraction of the total mass in the form of neutron stars varies from 0.0 to 4% , whereas the fraction of the total mass in the form of white dwarfs varies from 9 to 26% , depending on the model.

From a structural point of view, NGC 1835 appears rather concentrated, with values of the concentration parameter $c = \log(r_t/r_c)$ ranging from 1.81 to 2.24 (similar to 47 Tuc). It is worth mentioning that the size of NGC 1835 ($r_t \approx 50 \text{ pc}$) is quite comparable with the size of $\omega \text{ Cen}$ and 47 Tuc.

Depending on the model, the values obtained for the total mass of the cluster range from 0.70 to $1.55 \cdot 10^6 M_\odot$, with a representative mean total mass $\langle M_{\text{tot}} \rangle = 1.0 \cdot 10^6 M_\odot$. From Table 1, we see that the best results obtained by transforming the tidal radius r_t into mass (under the assumption of systemic rotation of the old globular cluster system) are smaller than the results from King-Michie models by about a factor of ten.

The half-mass relaxation time and the central relaxation time are of the order of 10 Gyr , and 10^7 yr respectively, allowing a large fraction of the central parts of the cluster to have been relaxed. Both isotropic and anisotropic models are successfully fitted to NGC 1835. A real velocity dispersion profile, instead of presently only the central value, would allow perhaps a better evaluation of the quantity of anisotropy.

The central surface brightness μ_0 varies from 6.53 to $6.72 \text{ mag/arcmin}^2$ with a representative mean value $\langle \mu_0 \rangle = 6.66 \text{ mag/arcmin}^2$. The integrated visual magnitude V_t varies from 9.85 to 9.91 mag with a representative mean value $\langle V_t \rangle = 9.88 \text{ mag}$. This last model value is situated between the observed values: $V_t = 9.48$ (Chun 1978), $V_t = 9.52$ (Elson and Freeman 1985), and $V_t = 10.13$ (van den Bergh 1981). The global mass-to-light ratio M/L_V varies from 2.50 to 5.21 , with a representative value $\langle M/L_V \rangle = 3.4$, whereas the central mass-to-light ratio $(M/L_V)_0$ varies from 1.93 to 2.63 . These values of the mass-to-light ratio are the direct consequences of the central value of the velocity dispersion, and depend also mainly on the mass function exponent x and on the quantity of anisotropy of the velocity dispersion.

5. A Universal M/L_V for Old Globular Clusters?

The present results (using King-Michie models) concerning the total

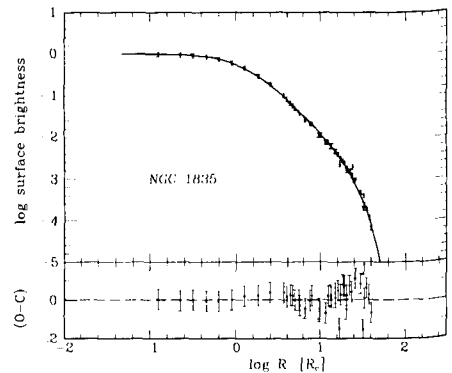


Figure 3: NGC 1835: logarithm of the observed (dots) and model surface brightness profiles as a function of the logarithm of the radius.

mass of NGC 1835 are larger than the best previous determinations (not using King-Michie models) by about a factor of ten, giving to this old LMC globular cluster a M/L_V ratio similar to those obtained for galactic globular clusters (Table 1). Consequently, the method based on the assumption of circular orbit (due to rotation) and on the transformation of the tidal radius into mass should be used only with great care in the case of Magellanic clusters. The systematic difference observed between the typical mass of rich globular clusters in the Galaxy (greater than $10^5 M_\odot$) and in the Magellanic Clouds (less than $10^5 M_\odot$) could be a simple artifact, a direct consequence of the idiosyncrasies of the different methods used.

In conclusion, when the same kind of dynamical models (King-Michie) constrained by the same kind of observations (surface brightness profile and central value of the velocity dispersion) are applied to an old rich Magellanic globular cluster, viz. NGC 1835, the results seem similar to those obtained in the case of 47 Tucanae. Consequently, the rich old globular clusters in the Magellanic Clouds could be quite similar (in mass and M/L_V) to the rich globular clusters in the Galaxy. The present study will be extended to as many Magellanic clusters as possible.

References

- Baranne, A., Mayor, M., and Poncet, J.-L. 1979, *Vistas in Astronomy*, **23**, 279.
- Chun, M.S. 1978, *Astron. J.*, **83**, 1062.
- Elson, R.A.W., and Freeman, K.C. 1985, *Astrophys. J.*, **288**, 521.
- Freeman, K.C. 1974 ESO/SRC/CERN Conference on Research Prog. for the New Large Telesc. Geneva p. 177.
- Griffin, R.F. 1967, *Astrophys. J.*, **148**, 465.
- Gunn, J.E., and Griffin, R.F. 1979, *Astron. J.*, **84**, 752.
- Lupton, R., Gunn, J.E., and Griffin, R.F. 1985 *Dynamics of Stars Clusters* IAU Symp.

113, Princeton 1984, Edit. J. Goodman and P. Hut, p. 19.
Lupton, R., Gunn, J.E., and Griffin, R.F. 1987, *Astron. J.*, **93**, 1114.
Mateo, M. 1987 Ph. D. Thesis University of

Washington.
Meylan, G. 1987, *Astron. Astrophys.*, **184**, 144.
Meylan, G. 1988a, *Astron. Astrophys.*, **191**, 215.

Meylan, G. 1988b, *Astrophys. J.*, **331**, 718.
Meylan, G. 1989, *Astron. Astrophys.* in press.
Pryor, C., McClure, R.D., Fletcher, J.M., Hartwick, F.D.A., and Kormendy, J. 1986, *Astron. J.*, **91**, 546.

High-tech Telescope on Top of Mount Wendelstein

H. BARWIG, *Universitäts-Sternwarte München, F.R. Germany*

A prominent feature of the silhouette of the Alps, the Wendelstein Mountain, can be seen from Garching on clear days. Extremely transparent skies sometimes even allow one to recognize on top of that mountain the domes of the Observatory of the University of Munich (USM). Only 75 km away, after one hour's ride, this site can easily be reached via cable car or by means of a famous 75-year-old cog railroad. Final access to the very top is achieved by an elevator climbing up 114 m within the mountain.

This Observatory had already a long tradition in solar research. First observations were started in 1940 (however, near the end of World War II they merely served the military to forecast radio disturbance caused by solar activity). Later, observations of solar prominences and of the solar corona began. After integration of the Observatory into the world-wide activities during the "International Geophysical Year" a 20-cm Zeiss Coudé Coronagraph was installed; it was used since 1963 to provide data for international solar research.

About 20 years later, when corona observations were reduced to only a few days a year due to increased air pollution, these activities had to be stopped: it was high time to think about the future of the Wendelstein Observatory. On the other hand, a statistical evaluation of weather data obtained over 7 years clearly indicated favourable conditions, at least for stellar observations, on about 145 days a year and fairly good seeing quality as well.

Thus in 1983 a new concept was elaborated to adapt the facilities to night-time observations and to move the solar instruments to a site on the Canary Islands. After many struggles for the required financial support, finally the green light was given to the telescope builder DFM Engineering in Colorado to provide an 90-cm fork-mounted Ritchey-Crétien telescope and auxiliary equipment, including a grating spectrograph and a CCD camera with an image data analysis system.

Construction work for the new dome building (Fig. 1) started in autumn 1987.

The telescope itself was delivered in November 1988, packed into a huge container that arrived at the bottom of Wendelstein after a journey of about 9,000 km. Helicopter flights scheduled for transportation to the mountain top had to be cancelled due to heavy snows and wind velocities up to 200 km/h. Therefore all of the equipment had to be brought up to the top using the cog railroad and two elevators.

The mechanical and optical setup was achieved within the scheduled time, although some problems were encountered in getting the telescope drive system to work because of strong signals from the nearby radio station. Extensive shielding measures finally solved this problem. "First light" through the telescope could be announced on January 18, 1989 when radiation reflected from Jupiter first passed through the new instrument.

However, long before this date our request to ESO concerning support of optical tests on the planned telescope had been answered positively – another example of the fruitful cooperation and of the mutual exchange of experience we had enjoyed with ESO in the past. For test purposes the ESO-Shack-Hartmann camera "ANTARES" could be

made available just before this instrument had to be shipped to Chile for application as wavefront sensor at the NTT. The Hartmann exposures will serve to perform the final optical alignments and to determine the overall optical quality. Prior to the completion of these tasks visual observations have already yielded a surprising result: The atmospheric conditions on Wendelstein during several test nights yielded seeing disks well below 1" (Craters on the Moon about one arcsec of diameter still showed shadow structures in their centres!).

The probability of having such favourable atmospheric conditions as well as the number of useful nights promised by weather statistics seem to justify the installation of such a high-tech telescope. Its performance differs in several respects from those of conventional instruments of comparable size: The thin primary mirror of accordingly low heat capacity is supported by an airbag. Its pressure is adjusted according to the mirror's weight on three hard points. This device guarantees preservation of the mirror's shape and therefore optimal image quality regardless of the telescope position. Furthermore the lightweight mirror allows a very stiff mount-



Figure 1: Ready for observation: the new telescope on Mount Wendelstein.